Rapid synthesis of tin oxide decorated carbon nanotube nanocomposites as anode materials for lithium-ion batteries

Jeng-Yu Lin *, Ming-Hung Chou, Yi-Chen Kuo

Department of Chemical Engineering, Tatung University, No. 40, Sec. 3, ChungShan North Rd., Taipei City 104, Taiwan

ABSTRACT

In this study, the tin oxide decorated carbon nanotubes (SnO_2–CNTs) nanocomposites have been successfully synthesized using an ultrafast and environmentally friendly microwave-assisted hydrothermal method. According to X-ray diffraction pattern, field emission scanning electron microscopy and transmission electron microscopy, the SnO_2 nanoclusters can directly grow on the surfaces of CNTs with uniform coverage along the longitudinal axis by using glucose as a binding agent. The electrochemical properties of the SnO_2–CNTs nanocomposite electrode have been further characterized by galvanostatic discharge/charge cycling tests, cyclic voltammetry and electrochemical impedance spectroscopy. Results demonstrate that the SnO_2–CNTs nanocomposite electrode exhibited a superior reversible discharge capacity, cycling stability and rate capability as an anode material for Li-ion batteries compared to the pristine SnO_2 electrode. Such synergic improvements can be attributed to combining the SnO_2 nanoclusters onto the conductive CNTs matrix by taking advantage of the relatively high specific capacity of SnO_2 nanoclusters and the excellent cycling capability of the CNTs.

© 2013 Elsevier B.V. All rights reserved.

1. Introduction

Lithium-ion batteries (LIBs) have attracted a lot of attention for applications in electric vehicles and portable electronic devices due to their higher energy density, stable cycling, environmental-friendly characteristics and high electromotive force for applications such as [1–3]. In general, graphitized carbon materials including natural graphite and mesocarbon microbeads (MCMB) have been widely used as anode materials for LIBs. These graphitized carbon anode materials have demonstrated their unique characteristics of outstanding cyclic calendar life, low irreversible capacity, stable structure, and low price. Nevertheless, because of the limited reversible capacity and power performances of graphitic carbons, advanced anode materials are urgently demanded for LIBs. In recent years, tin oxide (SnO_2) has been considered as an alternative anode material due to its high theoretical reversible capacity (782 mA h g^{-1}) [4,5]. However, the practical application of SnO_2 is restrained by the tremendous capacity decay during repeated charge/discharge cycles due to its huge volume change during Li$^+$ insertion and extraction processes. Such change in volume could result in polarization and poor electrical contact with the current collectors, thus limiting the cyclability of the metal or metal oxide base electrodes [6–11].

Consequently, nanostructured SnO_2 materials in the forms of hollow spheres, nanotubes, nanowires, nanorods, and mesoporous structures [12–15], have been designed to solve this issue. Nevertheless, the nanostructured SnO_2 still suffers from capacity fading and the cyclability of SnO_2 needs to be improved [16–19]. Thus, another inspiring strategy is to incorporate other phases, typically various forms of carbonaceous materials, to form SnO_2-based composites, such as SnO_2/graphite [20,21], SnO_2/MCMB [22], SnO_2/carbon nanotubes (CNTs) [23–25] and SnO_2/graphene [26–28]. The incorporation of these carbonaceous materials could not only improve the electrical conductivity of the SnO_2 composites, but also effectively alleviate the magnitude of volume expansion during the alloying and de-alloying cycles with Li$^+$, therefore possibly improving the electrochemical performance of SnO_2 composites to a large extent.

Among them, SnO_2/CNTs composites have attracted much interest as anode materials for LIBs because CNTs can form a three-dimension electric network and possess high surface-to-volume ratio, remarkable thermal conductivity, and good mechanical properties, which can be expected to restrain the volume expansion or the polarization of electrodes. Up to now, SnO_2 decorated onto the surface of CNTs to form SnO_2–CNTs composites for LIBs have been synthesized by the sol–gel method, chemical solution route, supercritical fluid method, chemical vapor deposition, and solvothermal method [29–33].

Most of them; however, the distribution of SnO_2 nanoparticles decorated on the CNTs was uneven. In this study, we reported a

facile procedure to synthesize SnO$_2$–CNTs nanocomposites as anode materials for LIBs through a microwave-assisted hydrothermal method with glucose as a binding agent. The use of microwave irradiation can uniformly heat the reactants to a high temperature within a short time, thus facilitating the mass production in a short time with relatively low energy cost [34–36]. Preliminary experimental results in this study demonstrate that the SnO$_2$–CNTs nanocomposite presented an improved reversible capacity and more excellent cycling ability in comparison with the pristine SnO$_2$ as anode material for LIBs.

2. Experimental

2.1. Preparation of SnO$_2$–CNTs nanocomposites

SnO$_2$–CNTs nanocomposites were synthesized by dissolving 0.07 M SnCl$_2$ (Acros, 98%) in 40 ml deionized water with 0.4 g glucose and then adding acid-treated multi-walled CNTs (Golden Innovation Business CO., Ltd. with a purity >99.5%). The nanocomposite was prepared with the molar ratios of SnCl$_2$ to CNTs of 1:3. The resultant aqueous solution was further dispersed by ultrasonication for 1 h, and then transferred into a microwave tube and kept at 200 °C with a microwave irradiation power of 700 W for 10 min. For comparison, the pristine SnO$_2$ or the mixture of SnO$_2$ and CNTs (SnO$_2$/CNTs) was also prepared by the similar method that described above, but without the addition of CNTs or glucose. After the microwave-assisted hydrothermal synthesis, the both resulting samples were washed with deionized water several times and collected by centrifuge treatment. Then, the samples were obtained at 60 °C overnight in a vacuum oven.

2.2. Material characterizations

The crystal structures of the SnO$_2$ and SnO$_2$–CNTs nanocomposite were characterized by X-ray diffraction (XRD-6000, Shimadzu Corporation, Japan) using a diffractometer with Cu Kα radiation (λ = 1.5406 Å), operated at 40 kV and 30 mA. The size and morphology of as-synthesized samples were observed by using scanning electron microscope (FESEM, JSM-7600F) and transmission electron microscopy (TEM, JEOL2010) equipped with an energy dispersive spectrometer (EDS). Thermogravimetric analysis (TGA) was performed by means of Pyris 1 TGA (Perkin Elmer) from room temperature to 900 °C in air at a heating rate of 5 °C min^{-1}.

2.3. Electrochemical measurements

The electrochemical properties of the as-synthesized samples were investigated using coin cells, as described in our previous study [37]. In brief, the synthesized samples were mixed with polyvinylidene fluoride binder (Kynar 740, ELF) and acetylene black (99.99%, Strem Chemicals Inc.) at the weight ratio of 80:10:10, and then ground along with adequate amount of N-methyl-2-pyrrolidone (ultra, ISP Technologies Inc.) as solvent for 1 day to form uniform slurry. The resultant slurry was coated onto a Cu foil (25 μm) by tape-casting method and then subjected to be dried under vacuum at 120 °C for 12 h to remove the residual solvent. After that, the foil was cut into disks with the diameter of 10 mm and pressed. The R2032 coin-type cells were assembled in an argon-filled glove box with a lithium metal as the counter electrode, a mesoporous membrane (Celgard 2500) as separator, and a mixed solvent of ethylene carbonate and dimethyl carbonate (1:1 in volume) containing 1 M LiPF$_6$ as electrolyte. The galvanostatic charge–discharge tests were carried out at a constant cut-off voltage of 0.005–2 V at different charge–discharge current densities using a home-made battery tester at ambient temperature. Cyclic voltammetry (CV) was performed by a computer-controlled electrochemical analyzer, CHI 614D (CH Instrument). Electrochemical impedance spectroscopy (EIS) analysis was performed using an IM-6 impedance analyzer (Zahner). EIS analysis was conducted at zero bias potential and the impedance data covered a frequency range of 0.1 Hz–1 MHz. The amplitude of the sinusoidal AC voltage signal was 5 mV. The complex nonlinear least square (CNLS) analyses of the resulting impedance spectra were conducted by means of the software, ZSimpWin version 3.1.

3. Results and discussion

Fig. 1 illustrates the XRD patterns of as-synthesized SnO$_2$ and SnO$_2$–CNTs nanocomposite. It can be found that all diffraction peaks in the pristine SnO$_2$ are assigned to the tetragonal crystalline structure (JCPDS No. 41-1445). As for the SnO$_2$–CNTs nanocomposite, the diffraction peaks at 26.7°, 33.9°, 38°, and 39° can correspond to the contribution of SnO$_2$ powders. Nevertheless, it can be apparently found that the peak at 26.7° for the SnO$_2$–CNTs nanocomposite is broader than that of the pristine SnO$_2$. This could
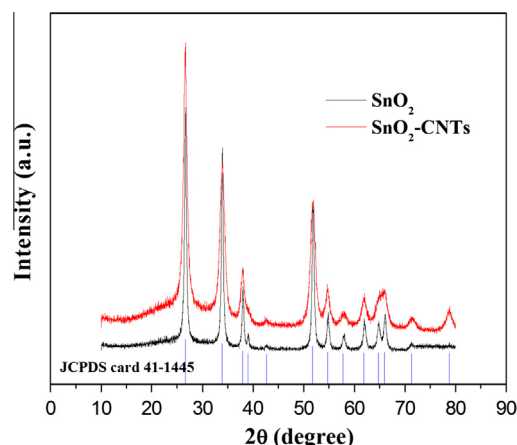

Fig. 1. XRD patterns of the as-synthesized pristine SnO$_2$ and SnO$_2$–CNTs powders.

be the reason that the peaks for CNTs (at 26°) and SnO$_2$ (at 26.7°) are so close that those two peaks are overplayed together to form an asymmetric broad peak, indicating the incorporation of CNTs in the nanocomposite.

Fig. 2a–c presents the FESEM images of the CNTs, pristine SnO$_2$ and SnO$_2$–CNTs nanocomposite. Fig. 2a shows the smooth outer walls of the CNTs with the diameter of around 75 nm and lengths of several micrometers. Fig. 2b reveals that the pristine SnO$_2$ particles aggregate into large particles with the particle size of about 100-400 nm. As shown in Fig. 2c, for the sample of SnO$_2$–CNTs synthesized in the presence of glucose, it is obvious that the as-synthesized SnO$_2$–CNTs nanocomposite still demonstrates one-dimensional structure with a significantly increased diameter of ∼150 nm compared to that of CNTs. This signifies that the CNTs are fully coated with smooth and uniform SnO$_2$ layers, and without any cracks and broken segments. However, if the precursor solution was absence of glucose, a mixture of CNTs and SnO$_2$ particles was obtained (Fig. 2d), in which SnO$_2$ particles is not uniformly deposited on the surfaces of CNTs. Thus, the CNTs seem to act as the conducting paths for connecting discrete SnO$_2$ particles. These results reveal that glucose plays a crucial role to form the SnO$_2$–CNTs nanocomposites. It is suggested that glucose seems to act as a binding agent to assist the SnO$_2$ nanoclusters formed on the surfaces of CNTs with uniform coverage along the longitudinal axis.

To further characterize the morphology of SnO$_2$–CNTs nanocomposites, TEM analysis was carried out. In the low-magnification TEM image (Fig. 3a), it can be observed that the lots of SnO$_2$ nanoclusters are uniformly decorated on the outside walls of the CNTs. Fig. 3b reveals that SnO$_2$ nanoclusters decorated on the CNTs are highly crystalline and the average particle size is approximately 4–5 nm. The aligned lattice fringes of the SnO$_2$ nanoclusters and CNTs are clearly illustrated in the high-resolution TEM (Fig. 3c), with adjacent fringe spacing of about 0.332 nm corresponding to the (1 1 0) plane of SnO$_2$. The corresponding ring-like selected-area electron diffraction (SAED) pattern (the inset in Fig. 3c) indicates that the nanostructures are polycrystalline and the diffraction rings from inside to outside can be indexed to (1 1 0), and (1 0 1) planes of rutile SnO$_2$, respectively. Fig. 3d presents the EDS result of the SnO$_2$–CNTs nanocomposites. Obviously, O and Sn elements are detected and can be ascribed to the SnO$_2$ nanoclusters, while the C element is possibly derived from CNTs. These results reveal that the SnO$_2$ nanoclusters are successfully decorated onto the surface of CNTs, which is consistent with the aforementioned results from FESEM and XRD analyses. As estimating the loading of SnO$_2$ nanoclusters in the SnO$_2$–CNTs nanocomposite, TGA analysis of the nanocomposite from room temperature to 900 °C in air at a heating rate of 5 °C min^{-1} was conducted since CNTs can be burned away over